Dalton Transactions

ROYAL SOCIETY OF CHEMISTRY

PAPER

View Article Online
View Journal | View Issue

Cite this: *Dalton Trans.*, 2023, **52**, 14400

Cooperative effects of Schiff base binuclear zinc complexes on the synthesis of aliphatic and semi-aromatic polyesters†

Federica Santulli, ‡ Federica Tufano, ‡ Mariachiara Cozzolino, Ilaria D'Auria, Maria Strianese, Mina Mazzeo and Marina Lamberti *

Received 26th July 2023,
Accepted 17th September 2023

DOI: 10.1039/d3dt02396f

rsc.li/dalton

In this paper, we use mono- and bimetallic complexes based on Earth-abundant, cheap and benign zinc for the synthesis of sustainable aliphatic and semi-aromatic polyesters. Tridentate and hexadentate aldimine-thioetherphenolate ligands were used to obtain the desired zinc complexes by the reaction of proligands with opportune equivalents of zinc bis[bis(trimethylsilyl)amide]. The obtained bimetallic complexes **1** and **2** and the monometallic complex **3** were used as catalysts in the Ring-Opening Polymerization (ROP) of landmark cyclic esters, such as ε-caprolactone and lactide, and in the Ring-Opening COPolymerization (ROCOP) of cyclohexene oxide and phthalic anhydride under different reaction conditions. All catalysts were active in these two classes of reactions, showing good control of the polymerization processes. Interestingly, the bimetallic complexes have higher activity compared to their monometallic counterparts, highlighting the cooperation between the two zinc centers.

Introduction

The accumulation of plastic waste in the environment causes hazardous effects, especially on marine wildlife, which is a considerable concern.[1] Consequently, there is growing interest directed both in the preparation of new polymeric materials that can be more sustainable for the environment,[2,3] and in the recycling of traditional polymers.[4]

Polyesters are amongst the most widely applied oxygenated polymers. Poly(ethylene terephthalate) (PET) is an aromatic polyester which makes up about 8% of world polymer production and it is found in applications spanning packaging, fibers, rigid plastics and engineering materials. PET is highly resistant to biodegradation; however, it is the most highly recycled resin.[5]

Aliphatic polyesters typically have lower physical and chemical properties compared to materials containing aromatic functionalities in the polymer backbone, for example, PET. However, aliphatic polyesters such as poly(ε-caprolactone) (PCL) and polylactide (PLA) have been attracting considerable attention as renewable and, in some cases, degradable alternatives to traditional polymers in biomedical, packaging, and agricultural fields.[6]

Currently, the catalytic Ring-Opening Polymerization (ROP) of cyclic esters is one of the most powerful and convenient methods for the preparation of aliphatic polyesters, allowing the synthesis of polymers with desired molecular masses and microstructures.[7] A more recent and less explored method is the sister polymerization method of Ring-Opening COPolymerization (ROCOP) of epoxides and cyclic anhydrides, which offers the opportunity to produce polyesters with a wide range of polymer backbone architectures, including aromatic/semi-aromatic, thanks to the large availability of structurally different starting monomers.[8]

Numerous metal complexes have been used to initiate the ROP of cyclic esters[9–12] and the ROCOP of epoxides and cyclic anhydrides,[13–15] in some cases displaying good catalytic activities with well-controlled characteristics. However, traces of residual metals in the polymers formed are very hard to remove completely and can be harmful to the environment or humans, consequently limiting their applications. The use of non-toxic metal ions in catalytic systems is one approach for solving this problem. Since zinc is one of the essential oligo-elements in the human body and has good biological activities, zinc-based metal catalysts are attracting increasing interest as green and biocompatible catalysts for such processes.[16] Zinc complexes with the general formula LZnX bearing various chelating organic ligands have been reported in the literature. Noteworthily, binuclear zinc complexes often show higher

Department of Chemistry and Biology "Adolfo Zambelli" University of Salerno, via Giovanni Paolo II, 132, 84084 Fisciano, SA, Italy. E-mail: mlamberti@unisa.it

†Electronic supplementary information (ESI) available. See DOI: https://doi.org/10.1039/d3dt02396f

‡These authors equally contributed to the paper.

activity or peculiar catalytic behaviors compared to their monometallic counterparts, thanks to the synergistic interactions between zinc atoms.[17–19] The most relevant examples of di-zinc complexes reported in the literature are supported by phenoxy-based ancillary ligands both for the ROP of lactide[20–30] and ε-caprolactone[31–35] and for the ROCOP of epoxides and cyclic anhydrides.[35–39]

As part of our research interest in zinc complexes in the ROP of cyclic esters,[40–44] we recently reported di-nuclear zinc complexes supported by properly designed bis(imino-pyridine) binaphthol ligands.[45] The cooperation of the zinc centers was highlighted at high polymerization temperatures, where the bimetallic system promoted the selective formation of low molecular weight cyclic polymers by back-biting reactions, while its monometallic counterpart was not able to promote the same process. In 2020, we synthesized mono- and bi-metallic zinc amido complexes supported by a new class of aldimine-thioether-phenolate ligands, which were active in the fixation of CO_2 with cyclohexene oxide, furnishing polycyclohexene carbonate when acting as single component catalysts. Whereas, the selctivity switched towards the formation of cyclohexene carbonates, when PPNCl was added as the cocatalyst to the reaction medium.[46] In logical continuation of this work, we decided to evaluate the performance of this class of zinc complexes as catalysts both for the ROP of landmark cyclic esters, such as ε-caprolactone and lactides, and for the ROCOP of cyclohexene oxide and phthalic anhydride, in order to prepare sustainable aliphatic and semi-aromatic polyesters, respectively.

Results and discussion

Synthesis of complexes 1–3

The general strategy for the synthesis of zinc complexes **1–3** is reported in Scheme 1. The reactions were carried out by following previously reported procedures.[46] ^{1}H NMR spectra (Fig. S1–S3†) confirmed the formation and the purity of all the synthesized compounds.

Since complexes with tetracoordinate zinc have a certain tendency to form dimeric species in solution in which the zinc increases its coordination number to five or six, in addition to the previous characterization experiments, the 2D version of the PGSE experiment (DOSY, diffusion ordered spectroscopy) was also performed to evaluate the diffusion coefficient (D) and then the nuclearity of complex **3** in solution (Fig. S4†). Using TMS as the internal standard in a C_6D_6 solution, the experimentally determined values of D were 1.56×10^{-9} m^2 s^{-1} for TMS and 5.76×10^{-10} m^2 s^{-1} for complex **3** (determined as the average of the values obtained for the different peaks of the zinc complex). Considering that the molecular mass (MM) of TMS is 88.23 g mol^{-1}, we estimated[43,45] an MM of 647 g mol^{-1} for the zinc complex (see the ESI for further details†), which is in good agreement with a theoretical value of 622.38 g mol^{-1}, thus indicating that complex **3** is stable as a monomeric species in solution.[47]

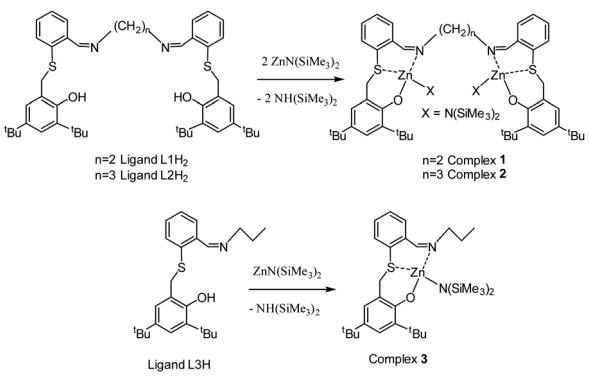

Scheme 1 Synthesis of the zinc complexes **1–3** from proligands.

Ring-opening polymerization of lactides

The ROP of L-lactide (L-LA) (Scheme 2) catalyzed by zinc complexes **1–3** was examined both in the absence and in the presence of isopropyl alcohol (^{i}PrOH) as a co-initiator by changing the temperature and solvent. Isolated polymeric samples were analysed by ^{1}H NMR spectroscopy and GPC techniques. Representative results are given in detail in Table 1.

Firstly, the behaviour of the zinc complexes with 100 equivalents of L-LA per Zn center was examined at 25 °C in the absence of a co-initiator. Under these conditions, the bimetallic complexes **1** and **2** showed very similar activities (*i.e.*, 76% and 69% of the converted lactide monomer for complexes **1** and **2**, respectively, in 24 hours), while the monometallic zinc complex **3** was the most active, converting 61% of L-LA in 9 hours. As expected, the catalytic activity enhanced with the increase of the polymerization temperature (entries 4–6 in Table 1), in all cases. For example, complex **1** led to 76% conversion of L-LA to the polymer in THF at 25 °C within 24 h (entry 1, Table 1), while it led to 86% conversion at 60 °C in 4 h (entry 4, Table 1). At 60 °C, complex **2** showed a double activity compared to complex **1** (*i.e.*, around 85% of L-LA monomer was converted in 4 hours for complex **1** and in 2 hours for complex **2**), while complex **3** was the most active with a conversion of 82% in 1 hour. However, for the bimetallic complexes **1** and **2**, the molecular weights of the polymers determined by GPC closely matched the calculated values both at 25 °C and 60 °C, while for the most active monometallic complex **3**, the experimental molecular weights were around three times higher than the calculated values, thus suggesting an initiation process slower than the propagation reaction. For the bimetallic complexes, the theoretical

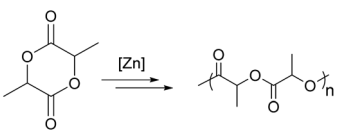

Scheme 2 General reaction for the ring-opening polymerization of lactides.

Table 1 Ring-opening polymerization of L-lactide by complexes **1–3**

Entry	Cat.	$[L\text{-LA}]_0 : [Zn]_0 : [^iPrOH]_0$	Temp (°C)	Time (h)	Conv.[a] (%)	M_n^{th} [b] ($\times 10^3$)	M_n^{GPC} [c] ($\times 10^3$)	$Đ$ [c]
1	**1**	200 : 2 : 0	25	24	76	21.9	21.1	1.17
2	**2**	200 : 2 : 0	25	24	69	19.9	21.0	1.27
3	**3**	100 : 1 : 0	25	9	61	8.8	34.4	1.34
4	**1**	200 : 2 : 0	60	4	86	24.8	28.8	1.24
5	**2**	200 : 2 : 0	60	2	85	24.6	24.7	1.23
6	**3**	100 : 1 : 0	60	1	82	11.8	31.3	1.47
7	**1**	200 : 2 : 2	25	0.5	31			
				3	71	10.2	7.3	1.07
8	**2**	200 : 2 : 2	25	0.5	75			
				1	90	13.0	11.4	1.17
9	**3**	100 : 1 : 1	25	0.5	18			
				3	67	9.7	6.5	1.09
10	**2**	200 : 2 : 4	25	0.5	61			
				1	83	6.0	7.3	1.35
11	**2**	800 : 2 : 10	25	0.5	27			
				1	53	6.1	3.7	1.38

General conditions: all reactions were carried out in 1 mL of THF. $[\mathbf{1}]_0$–$[\mathbf{2}]_0 = 5.0 \times 10^{-6}$ mol; $[\mathbf{3}]_0 = 1.0 \times 10^{-5}$ mol, (*i.e.*, $[Zn]_0 = 1.0 \times 10^{-2}$ M). [L-LA] = 1.0 M except in entries 11 and 12. [a] Determined by ^{1}H NMR spectral data. [b] M_n^{th} (g mol^{-1}) 144.13 × ($[L\text{-LA}]_0/[Cat]_0$) × L-LA conversion (for entries 1–6) and M_n^{th} (g mol^{-1}) 144.13 × ($[L\text{-LA}]_0/[^iPrOH]_0$) × L-LA conversion (for entries 7–11). [c] Experimental M_n (in g mol^{-1}) and M_w/M_n ($Đ$) values were determined by GPC in THF using polystyrene standards and corrected using a factor of 0.58.

molecular masses were calculated considering the growth of a single polymer chain per complex: reasonably, under these conditions, once the initiation in one of the metallic centers has taken place, the propagation of this polymeric chain is favoured compared to the initiation in the other zinc–amido bond. The polylactides (PLAs), produced by **1** and **2** under the described conditions, had relatively narrow molecular weight distributions (M_w/M_n) of 1.17–1.27. Moreover, by monitoring the molecular weights and molecular weight distributions of a PLA sample obtained using complex **2** as the catalyst, as a function of conversion, a linear increase in molecular weights *versus* PLA conversion was observed, while the molecular weight distribution remained almost constant (see Fig. S6 and Table S2 in the ESI†), thus suggesting that the catalytically active species was stable during the reaction and polymerization was well controlled. On the other hand, for complex **3**, the dispersity values were slightly higher (1.34 and 1.47 at 25 °C and 60 °C, respectively), as expected on the basis of the previous considerations on the initiation step rate.

Subsequently, one equivalent of isopropyl alcohol per metal center was added as a co-catalyst to the complexes to convert the labile amido ligands into generally more active alkoxide ligands. Upon the addition of isopropyl alcohol to the zinc complexes at 25 °C, all catalytic systems showed higher activities.[48] Interestingly, under these conditions, the order of activity was: **2** > **1** > **3** as well evident, for example, by comparing the conversion values of the three systems after a reaction time of 0.5 hours: 75%, 31% and 18% conversions were obtained, corresponding to TOF values of 150 h^{-1}, 62 h^{-1} and 36 h^{-1} for complexes **2**, **1** and **3**, respectively (entries 7–9 in Table 1). In particular, the higher activity of the bimetallic complexes **1** and **2** compared to their mononuclear analogues suggests that a cooperative mechanism may be in effect. Moreover, the conversion values, approximately double for complex **2** compared to complex **1**, indicate that the bridge length between the nitrogen atoms, which influences both the distance between the zinc centers and the fluxionality of the complexes, is a critical parameter in the cooperativity between the two metal centers.[49]

Under these conditions, the experimental molecular weights were in good agreement with the theoretical molecular weights for the three complexes, and the low dispersity values indicated a controlled chain growth. In the presence of ^{i}PrOH, the theoretical molecular weights were calculated taking into account the number of monomer equivalents compared to the alcohol equivalents, according to the formula reported in the literature by various authors[22,28] and specified in the footnote "*b*" of Table 1.

As observed in the polymerization process carried out with complex **2** in the absence of a co-initiator, also for the catalytic system constituted by complex **2** and isopropanol, a linear increase of molecular weights compared to PLA conversion, and almost constant molecular weight distributions (Fig. S7 and Table S3 in the ESI†) underlined the good control of the polymerization process.

To get more information on the nature of the active species for the polymerization experiments in the presence of the alcohol, an alcoholysis experiment was carried out by adding 2 equivalents of isopropyl alcohol to the solution of the bimetallic complex **2** in deuterated benzene as solvent. By studying the ^{1}H NMR spectrum (Fig. S8 in the ESI†) of this reaction mixture, we observed the formation of a new species, as indicated by significant variations of all the chemical shift values compared to the signals of complex **2** alone (comparing Fig. S2 and S8 in the ESI†). Most importantly, we observed the disappearance of the amido signal and the appearance of the signal due to the free amine, indicating the reaction of isopropyl alcohol with both the amido groups. This result was also supported by the integration values of the signals due to the isopropoxide groups. Thus, the alcoholysis experiment con-

firms the formation of a new species with two alkoxide groups replacing the two amido groups.

The behaviour of the most active complex **2** was also explored in the presence of an increased number of equivalents of initiator and/or monomer (entries 10 and 11 in Table 1). The activity remained high and a good control of the molecular mass was also observed under these conditions.

The PLA sample obtained in the polymerization experiment of entry 10 was also studied by NMR spectroscopy and MALDI time-of-flight mass-spectrometry (MALDI-TOF-MS) analyses. The ^{1}H NMR spectrum of this sample clearly shows the existence of $HOCH(CH_3)CO–$ and $–OCH(CH_3)_2$ groups as exclusive chain end groups (Fig. S9 in the ESI†). This supports the hypothesis that the polymerization follows a coordination–insertion mechanism and is initiated by the transfer of an alkoxide group to the monomer. The MALDI-TOF analysis (Fig. S10 in the ESI†) confirmed the observed end groups and showed that only linear oligomers with integral LA repeat units were formed, suggesting that inter- and intramolecular transesterification processes did not occur during the polymerization process.

The more encumbered bimetallic complexes **1** and **2** were subsequently used as catalysts in the ROP of *rac*-LA at 25 °C and in the absence of the co-catalyst (for more details see entries S1 and S2 in Table S4†). The activities were close to those obtained in the ROP of L-LA under the same conditions, and the experimental number-average molecular weights were in agreement with the calculated values, also suggesting a controlled polymerization process when the racemic mixture of lactide enantiomers is polymerized. However, an atactic microstructure was revealed by the homo decoupled ^{1}H NMR spectra of the methine regions of PLAs: the discrepancy between the experimental intensities of the peaks due to different tetrads, with the theoretical values calculated by assuming both an enantiomorphic site control and a chain end control, further confirmed that no control of the polymer microstructure it is active under these conditions (see, for example, Fig. S11 and Tables S5 and S6 in the ESI†).

Finally, we explored the effect of the solvent on the polymerization outcome (Table S7†). The behaviour of complex **2** in L-LA polymerization was studied in toluene and dichloromethane and the results were compared with those obtained in more polar and more coordinating tetrahydrofuran (to help readers with comparisons, entries 2 and 5 of Table 1 were also reported in Table S7†). The polymerization experiment carried out in dichloromethane at 25 °C showed similar activity to that obtained in THF (entry 2 *vs.* S3†). Due to the lower solubility of L-LA in toluene, this polymerization was conducted at 60 °C. In comparison with the same experiment in THF, the activity was lower, although we observed that the solubilisation of the monomer was not complete under these conditions. For this reason, we conducted two new polymerizations by increasing the solvent amount to 2.5 mL (corresponding to a decrease in concentration from $[LA]_0$ = 1.0 M to 4.0 × 10^{-1} M). Under these more dilute conditions, the conversion of L-LA was quite the same in both solvents, at all times when withdrawals were made (entries S5 *vs.* S6†).

In summary, from the results of the polymerization tests, we can hypothesize that for the amide species of the bimetallic complexes **1** and **2**, there is no cooperation between the metal centers, and under these conditions, the polymerization process is faster for the less sterically encumbered monometallic complex **3**. In contrast, the structures of alkoxy derivatives allow a cooperative interaction between the two zinc centers of the bimetallic complexes, ensuring greater activity compared to their monometallic counterpart. Furthermore, the length of the bridge between the two imine nitrogen atoms appears to be a key parameter, with the propylene bridge of complex **2** guaranteeing an activity about double than that observed with complex **1** with the ethylene bridge.

Ring-opening polymerization of ε-caprolactone

Although ε-caprolactone (ε-CL) is industrially produced from non-renewable resources, *i.e.*, by Baeyer–Villiger oxidation of cyclohexanone derived from petro-derived cyclohexane or phenols, promising and more sustainable strategies have been outlined. In fact, the synthesis of cyclohexanone from lignin-derived aromatic ethers has been described, while ε-caprolactone itself has been obtained by oxidative lactonization of 1,6-hexanediol.[50,51] Thus, poly-ε-caprolactone (PCL) can also be classified into sustainable polymers with full rights, as it is biodegradable and can be obtained from renewable sources.

Zinc complexes **1–3** were assessed by the polymerization of ε-caprolactone (Scheme 3) and representative results are summarized in Table 2. The obtained polymers were characterized by NMR, GPC and MALDI-TOF analyses. All complexes showed good activity, allowing the conversions of 100–400 equiv. of ε-caprolactone at room temperature.[52]

The activity of the bimetallic complexes **1** and **2** in the ring-opening polymerization of ε-caprolactone was evaluated in THF solution at room temperature in the presence of one equivalent of ^{i}PrOH per metallic center and with both 100 and 200 monomer equivalents per zinc center. Under both conditions, complex **1** was found to be more active than complex **2**, showing a maximum TOF of 216 h^{-1} (entry 12 in Table 2). Monometallic complex **3**, under the same conditions with 100 equivalents of the monomer, showed lower activity than the bimetallic counterparts. Thus, for ε-caprolactone polymerization, the order of activity was **1** > **2** > **3**, as deducible from the conversions after 0.5 hours under the same reaction conditions: 54%, 27% and 14% for complexes **1**, **2** and **3**, respectively (entries 12, 14 and 16 in Table 2), indicating that also for the ROP of this monomer, the cooperativity between the metallic centers increases the activity. However, a reversal of reactivity between complex **1** and complex **2** was observed when com-

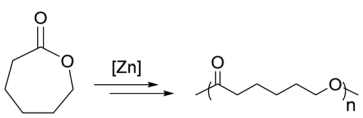

Scheme 3 General reaction for the ring-opening polymerization of ε-caprolactone.

Table 2 Ring-opening polymerization of ε-caprolactone by complexes **1–3**

Entry	Cat.	$[\varepsilon\text{-CL}]_0 : [Zn]_0 : [^i\text{PrOH}]_0$	Solvent	Time (h)	Conv.[a] (%)	M_n^{th} [b] ($\times 10^3$)	M_n^{GPC} [c] ($\times 10^3$)	$Đ$[c]
12	**1**	400 : 2 : 2	THF	0.5	54			
				2	92	21.0	21.8	1.41
13	**1**	200 : 2 : 2	THF	0.5	53			
				1.5	88	10.0	7.8	1.51
14	**2**	400 : 2 : 2	THF	0.5	27			
				2	79	18.0	12.1	1.26
15	**3**	200 : 2 : 2	THF	0.5	18			
				2	89	10.1	5.9	1.31
16	**3**	200 : 1 : 1	THF	0.5	14			
				1.5	61	13.7	12.9	1.26
17	**3**	200 : 1 : 1	Toluene	0.5	63			
				1	80	18.3	17.2	1.16
18	**3**	200 : 1 : 1	CH_2Cl_2	0.5	18			
				3	79	18.0	18.2	1.16
19	**3**	200 : 1 : 0	Toluene	0.5	6			
				5	45	10.3	32.9	1.59

General conditions: all reactions were carried out in 2 mL of solvent. $[\mathbf{1}]_0$–$[\mathbf{2}]_0$ = 5.0 × 10^{-6} mol; $[\mathbf{3}]_0$ = 1.0 × 10^{-5} mol (*i.e.*, [Zn] = 5 mM). [a] Determined by ^{1}H NMR spectral data. [b] M_n^{th} (g mol^{-1}) = 114.13 × ([ε-CL] /[^{i}PrOH]) × ε-CL conversion. [c] Experimental M_n (in g mol^{-1}) and M_w/M_n ($Đ$) values were determined by GPC in THF using polystyrene standards and corrected using a factor of 0.56.

pared to lactide polymerization experiments, suggesting that the optimal length of the bridge for the most efficient cooperation between the metal centers also depends on the nature of the monomer.[53]

Fig. 1 displays a typical semilogarithmic plot of −ln[monomer]$_t$ *vs.* time, showing, as might be expected, a first-order polymerization reaction in ε-CL concentration. The determined rate constants (k_{obs}) were 1.3, 7.4 × 10^{-1} and 5.7 × 10^{-1} h^{-1} for complexes **1**, **2** and **3**, respectively.

Subsequently, we also explored the effect of the solvent on the polymerization of ε-caprolactone with complex **3** under the same reaction conditions (entries 16–18 in Table 2). In this case, while the activity in THF and dichloromethane was similar, a significant increase was observed in the less polar solvent, toluene.

In most of the cases, experimental molecular weights obtained by GPC analysis of PCLs were in good agreement with the theoretical values, indicating a good control of the polymerization process. As observed in L-lactide polymerization, for complex **3**, in the absence of the alcohol initiator, the polymerization slows down and the control of the molecular masses is lost (entry 19 in Table 2).

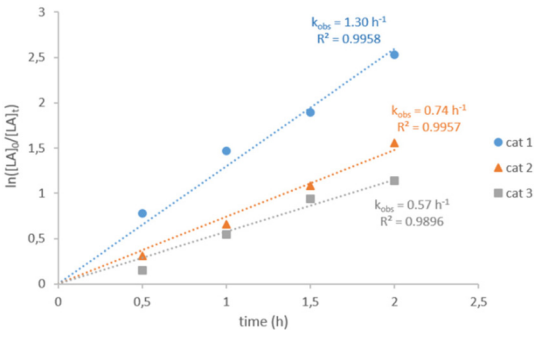

Fig. 1 First-order kinetic plots for the consumption of ε-CL in THF at 20 °C by complex **1** (blue circles, entry 12 in Table 2), complex **2** (orange triangles, entry 14 in Table 2) and complex **3** (grey squares, entry 16 in Table 2) in combination with ^{i}PrOH.

^{1}H NMR and MALDI-TOF analyses of the PCL sample obtained by the experiment detailed in entry 15 of Table 2 (Fig. S12 and S13 in the ESI†) clearly showed the existence of $HO(CH_2)_5CO$– and –$OCH(CH_3)_2$ as exclusive chain end groups, indicating that the ROP of ε-CL proceeds *via* a coordination–insertion mechanism pathway. The molecular weight calculated by integrating the signals in the ^{1}H NMR spectrum was in good agreement with those obtained by both MALDI and GPC analyses (M_n^{NMR} = 4860 g mol^{-1}, M_n^{MALDI} = 4890 g mol^{-1}, and M_n^{GPC} = 5900 g mol^{-1}), although it was lower than the theoretical molecular weight (M_n^{th} = 10 100 g mol^{-1}).

Ring-opening co-polymerization of phthalic anhydride and cyclohexene oxide

ROCOP of phthalic anhydride (PA) and cyclohexene oxide (CHO) allows the insertion of aromatic groups in the polymer backbone, a desirable goal to increase the thermal and mechanical properties of aliphatic polyesters obtainable by ROP. Phthalic anhydride and cyclohexene oxide are currently produced from petroleum derivatives, however, more sustainable synthetic strategies have been described: PA can be synthesized either from furan and maleic anhydride, or by cyclisation of dicarboxylic acids, all substrates are available from carbohydrates,[54,55] while CHO can be obtained from 1,4-cyclohexadiene, a waste by-product of plant oil self-metathesis.[56]

Thus, complexes **1–3**, in combination with different co-catalysts, were tested as catalysts in these copolymerization reactions (Scheme 4). The composition of the obtained polymers was estimated by ^{1}H NMR analysis, by comparing the integrals of the signals of epoxide/anhydride sequences with those of sequential enchainment of epoxides. The polymers produced were also characterized by GPC and MALDI-TOF analyses. The most relevant results are summarized in Table 3.

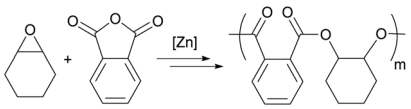

Scheme 4 General reaction for the ring-opening copolymerization of cyclohexene oxide and phthalic anhydride.

First, we explored the behavior of complex **1** at 110 °C in toluene as the solvent with a CHO/PA/catalyst ratio of 250 : 250 : 1 and 2 equivalents of co-catalyst. In these copolymerization reactions, the co-catalyst plays a double role, influencing both the activity and the selectivity of the process. Using ^{i}PrOH, TBAB (tetra-*n*-butylammonium bromide) and DMAP (4-(*N*,*N*-dimethylamino)pyridine) as the co-catalysts (entries 20–22 in Table 3), we found DMAP as the most efficient co-catalyst (84% of PA conversion after 16 h) and TBAB as the least (58% of PA conversion after 16 h). In addition, TBAB and DMAP gave the most selective catalytic systems; in fact, in both cases, copolymerization proceeded in an exclusive alternating fashion with an ester content linkage of >99%. Thus, we selected TBAB as the co-catalyst to compare the behavior of complexes **1–3** in this class of copolymerization reactions under the same reaction conditions (entries 22–24). By comparing the conversions after 16 hours of polymerization reaction, the three complexes showed the following order of activity: **1** > **2** > **3**, which is the same as that of ε-caprolactone polymerization. Thus, also in the ROCOP of PA and CHO, a cooperative effect between the two zinc centers may be in effect, with, in this case, a preference for the shortest ethylene bridge between nitrogen atoms, compared to the propylene bridge. Remarkably, both the monometallic complex and the bimetallic complexes were highly selective in the production of polyesters (for example, see Fig. S15 in the ESI†).

The GPC analysis of all obtained polyesters showed monomodal distributions with narrow dispersities ($Đ$ < 1.41; using DMAP as the cocatalyst $Đ$ < 1.25), indicating a controlled behavior of these catalytic systems in the ROCOP reactions. The number-average molecular weight values (M_n) measured by GPC were in most cases lower than the theoretical ones: this is a quite common situation in these copolymerization reactions and it is usually attributed to the presence of protic impurities, which act as chain transfer agents, such as the trace of water and/or diacid resulting from hydrolyzed anhydride.

Conclusions

In summary, in this paper, we focused on the synthesis of aliphatic and semi-aromatic polyesters derived from renewable resources, promoted by catalytic systems based on zinc, a biocompatible metal. Mono- and bi-metallic zinc complexes, bearing aldimine-thioetherphenolate ligands, have been used as catalysts in the ROP of lactides and ε-caprolactone and in the ROCOP of cyclohexene oxide and phthalic anhydride.

All complexes were active in the ROP of the selected cyclic esters using isopropylic alcohol as the co-catalyst, showing good control of molecular weights, narrow dispersities and end-group fidelity. In the ROCOP of CHO with PA, the three complexes, in combination with DMAP as the co-catalyst, provided polyesters with complete selectivity. Thus, the studied complexes were able to furnish both aliphatic and semi-aromatic polyesters, although with lower activities compared to the most active systems reported in the literature,[9–11,14,15] such as zinc complexes showing a TOF of up to 60 000 h^{-1} in the ROP of lactide[28] and 200 h^{-1} in the ROCOP of PA with CHO.[38] Keeping the concentration of the monomer and zinc centers strictly constant, we observed up to 4-fold enhancement of polymerization activity for the bimetallic complexes compared to the monometallic congener, highlighting cooperative effects provided by the two close metal centers.

Interestingly, the spacing between zinc atoms was found to be a key parameter for determining the order of activity, with an unexpected dependence on the polymerized monomers. In fact, the bimetallic complex **2**, supported by the ligand with a propylene bridge between the nitrogen atoms, showed the highest activity in the polymerization of L- and *rac*-lactide; the distance and fluxionality dictated by the ligand with the ethyl-

Table 3 Ring-opening copolymerization of cyclohexene oxide and phthalic anhydride by complexes **1–3**

Entry	Cat.	$[CHO]_0$: $[PA]_0$: $[Zn]_0$: $[cocat]_0$	Cocat.	Time (h)	Conv.[a] (%)	Ester content[b] (%)	M_n^{th} [c] ($\times 10^3$)	M_n^{GPC} [d] ($\times 10^3$)	$Đ$[d]
20	**1**	250 : 250 : 2 : 2	^{i}PrOH	24	92	78	28.3	8.1	1.41
21	**1**	250 : 250 : 2 : 2	TBAB	16	58	>99			
				24	76	>99	23.4	11.8	1.28
22	**1**	250 : 250 : 2 : 2	DMAP	16	84	>99	25.9	25.2	1.23
23	**2**	250 : 250 : 2 : 2	DMAP	16	70	>99			
				24	87	>99	26.8	14.5	1.25
24	**3**	125 : 125 : 1 : 1	DMAP	16	54	>99			
				24	67	>99	20.6	14.1	1.25

General conditions: $[\mathbf{1}]_0$–$[\mathbf{2}]_0 = 1 \times 10^{-5}$ mol; $[\mathbf{3}]_0 = 2 \times 10^{-5}$ mol; CHO = 2.5×10^{-3} mol (245 mg); PA = 2.5×10^{-3} mol (370 mg); toluene = 1 mL. Temperature: 110 °C. [a] Determined by ^{1}H NMR spectroscopy ($CDCl_3$) by integrating the normalized resonances for PA (7.97 ppm) and the phenylene signals in PE (7.30–7.83 ppm). [b] Determined by ^{1}H NMR spectroscopy ($CDCl_3$) integrating the normalized resonances for ester linkages (4.80–5.40 ppm) and ether linkages (3.28–3.86 ppm). See Fig. S14 in the ESI.† [c] M_n^{th} (g mol^{-1}) = 246.36 × ([PA]/[^{i}PrOH]) × PA conversion. [d] Experimental M_n (in g mol^{-1}) and M_w/M_n ($Đ$) values were determined by GPC in THF using polystyrene standards and corrected using a factor of 1.85.[57]

ene bridge make the bimetallic complex **1** the most active catalyst for both the ROP of ε-CL and the ROCOP of PA with CHO. Looking into the literature for the behavior of bimetallic complexes as catalysts, one can find different situations. In some cases, the smallest distances between the metals of binuclear complexes determine the greatest activity, suggesting that more efficient intermetallic cooperation contributes to higher activity.[28] In other cases, catalysts with shorter distances between metals show lower catalytic activity than those with longer distances, reasonably because the crowded environment around the metal centers may slow down or even hinder the polymerization process.[58] Our peculiar situation, where we observed that for the bimetallic complexes with different metal–metal distances, the order of activity depends on the monomers, could be explained on the basis of different steric hindrances and/or coordination modes of the explored monomers.[59] In fact, for the bulkiest lactide monomer, the greatest activity is recorded with the bimetallic complex **2** in which the metal centers are more spaced apart.

Experimental

General considerations

All reactions with substances that are sensitive toward air or moisture were carried out in dried glassware (24 h at 150 °C in an oven or 5 min at 650 °C in a vacuum) under a positive pressure of nitrogen (*ca.* 1.2 bar). Solvents and reagents were obtained from Merck and used as received unless stated otherwise. Methylene chloride, tetrahydrofuran, benzene, toluene, isopropyl alcohol and hexane used for polymerization experiments and the synthesis of substances unstable toward air and moisture, were distilled prior to use on an opportune drying agent. In particular, THF, toluene, benzene and hexane were dried by refluxing over sodium and benzophenone and stored under nitrogen. Dichloromethane and isopropanol were dried over calcium hydride and distilled prior to use.

Methanol, ethanol, *n*-hexane, and tetrahydrofuran (HPLC grade) were used without further purification.

The lactide monomers (L-LA and *rac*-LA) were crystallized in toluene and then dried over P_2O_5. Cyclohexene oxide (CHO) and ε-caprolactone were dried over CaH_2 and distilled under nitrogen. Phthalic anhydride was purified by dissolving it in toluene, filtering off impurities, recrystallizing and then subliming. All dry solvents and monomers were stored under nitrogen. Deuterated solvents for NMR experiments were stored at 20 °C over molecular sieves. NMR spectra were measured with 300/400/600 MHz Bruker AVANCE spectrometers at 20 °C. Chemical shifts δ are given in ppm relative to the residual solvent peak of the used deuterated solvent. Molecular masses (M_n and M_w) and their dispersities (M_w/M_n) were measured by gel permeation chromatography (GPC), using THF as the eluent (1.0 mL min^{-1}) and narrow polystyrene standards were used as the reference. MALDI-TOF mass spectra were recorded using a Bruker solariX XR Fourier transform ion cyclotron resonance (FT-ICR) mass spectrometer (Bruker Daltonik GmbH, Bremen, Germany) equipped with a 7 T refrigerated actively shielded superconducting magnet (Bruker Biospin, Wissembourg, France). The samples were prepared at a concentration of 1.0 mg mL^{-1} in THF, while the matrix (DCTB) was mixed at a concentration of 10.0 mg ml^{-1}.

Synthesis of complexes[46]

Synthesis of complex 1. To a benzene solution (6 mL) of $L1H_2$ (0.300 g, 4.06×10^{-4} mol), a benzene solution (3.0 mL) of $Zn[N(SiMe_3)_2]_2$ (0.314 g, 8.14×10^{-4} mol) was added. The reaction mixture was stirred at room temperature for 2 hours. Afterwards, the solvent was removed in a vacuum and the solid residue was washed with pentane. Complex **1** was obtained as a yellow powder in 90% yield. ^{1}H NMR (400 MHz, C_6D_6, 298 K): δ 8.62 (s, 2H, CH═N), 7.63 (d, J = 2.53 Hz, 2H, Ar–H), 7.60 (d, J = 7.88 Hz, 2H, Ar–H), 7.29 (br, 2H, Ar–H), 7.08 (d, J = 2.48 Hz, 2H, Ar–H), 6.58 (t, 2H, Ar–H), 6.49 (t, 2H, Ar–H), 4.98 (br, 2H, N–CH_2), 4.51 (br, 4H, S–CH_2), 3.57 (br, 2H, N–CH_2), 1.90 (s, 18H, CCH_3), 1.50 (s, 18H, CCH_3), 0.14 (br, 36H, $Si(CH_3)_3$).

Synthesis of complex 2. The same procedure used for complex **1** was followed using the ligand precursor $L2H_2$ (0.300 g, 4.00×10^{-4} mol) and $Zn[N(SiMe_3)_2]_2$ (0.318 g, 8.00×10^{-4} mol). Complex **2** was obtained as a yellow powder in 95% yield. ^{1}H NMR (400 MHz, C_6D_6, 298 K): δ 8.24 (s, 2H, CH═N), 7.80 (d, J = 7.92 Hz, 2H, Ar–H), 7.60 (d, J = 2.50 Hz, 2H, Ar–H), 6.80 (d, J = 2.15 Hz, 2H, Ar–H), 6.76 (m, 4H, Ar–H), 6.66 (t, 2H, Ar–H), 4.25 (br, 4H, S–CH_2), 4.00 (br, 4H, N–CH_2), 1.82 (s, 18H, CCH_3), 1.50 (s, 18H, CCH_3), 0.10 (s, 36H, $Si(CH_3)_3$).

Synthesis of complex 3. The same procedure used for complex **1** was followed using the ligand precursor L3H (0.300 g, 7.54×10^{-4} mol) and $Zn[N(SiMe_3)_2]_2$ (0.304 g, 7.54×10^{-4} mol). Complex **3** was obtained as a yellow powder in 93% yield. ^{1}H NMR (400 MHz, C_6D_6, 298 K): δ 7.84 (d, J = 7.90 Hz 2H, Ar–H), 7.73 (s, 1H, CH═N), 7.59(s, 1H, Ar–H), 7.05 (s, 1H, Ar–H), 6.75 (m, 3H, Ar–H), 3.98 (br, 2H, S–CH_2), 3.54 (br, 2H, N–CH_2), 1.83 (s, 9H, CCH_3), 1.49 (s, 9H, CCH_3), 0.78 (t, 3H, CH_3), 0.10 (s, 18H, $Si(CH_3)_3$).

Polymerization procedures

Lactide polymerization reactions. The polymerization experiments were carried out in a glove box. The complex was weighed and added to a 4 ml vial, fitted with a magnetic stirrer (5.0×10^{-6} mol for complexes **1** and **2** and 1.0×10^{-5} mol for complex **3**): subsequently, a solution of the co-catalyst (0.1 M of ^{i}PrOH in the reaction solvent) was added and stirred for 5 minutes. In a 4 mL vial, the monomer was weighed and dissolved in the same solvent. Finally, the monomer solution was added to the solution of the catalytic system. The polymerization experiments were stopped by taking the 4 ml vial out of the glove box and adding dichloromethane. The solvent was removed under reduced pressure, and the polymer was dried in a vacuum oven and characterized by NMR spectroscopy and GPC.

ε-Caprolactone polymerization reactions. The polymerization experiments were carried out in a glove box. The zinc complex was weighed (5.0×10^{-6} mol for complexes **1** and **2** and 1.0×10^{-5} mol for complex **3**) and added to a 4 ml vial,

fitted with a magnetic stirrer. Subsequently, a solution of the co-catalyst (0.1 M of ^{i}PrOH in the reaction solvent) was added and stirred for 5 minutes. In another 4 mL vial, the monomer was weighed and dissolved in the reaction solvent. Finally, the monomer solution was added to the first solution. The polymerization was stopped using dichloromethane after taking the vial out of the glove box. The solvent was removed under reduced pressure, and the polymer was dried in a vacuum oven and characterized by NMR spectroscopy and GPC analysis.

PA/CHO polymerization reactions. In a glove box, the previously weighed monomer and the co-catalyst were transferred into a 10 mL Schlenk tube, equipped with a magnetic stirrer, and dissolved in 0.5 ml of toluene. In a 2 mL vial, the complex (5.0×10^{-6} mol for complexes **1** and **2** and 1.0×10^{-5} mol for complex **3**) was weighed and dissolved in 0.5 mL solvent. Subsequently, the complex solution was transferred into the Schlenk tube: the latter was closed, taken out of the glove box and immersed in a thermostated oil bath at a temperature of 110 °C. The polymerizations were stopped after the prescribed time using dichloromethane. The solvent was removed under reduced pressure and the polymer was coagulated in methanol, filtered, dried in a vacuum oven and characterized by NMR spectroscopy and GPC analysis.

Author contributions

Conceptualization: M. L.; methodology: F. S., F. T., M. C. and I. D.; investigation: M. M. and M. S.; visualization: M. L. and F. S.; data curation: M. L.; writing – review and editing: M. L. and M. M. All authors have read and agreed to the published version of the manuscript.

Conflicts of interest

There are no conflicts to declare.

Acknowledgements

The authors thank Dr Patrizia Iannece for elemental analysis, Dr Patrizia Oliva for NMR technical assistance, and Dr Mariagrazia Napoli for GPC analysis. The authors are grateful for funding from the Università degli Studi di Salerno (FARB grant: ORSA210303) and open access funding provided by Università degli Studi di Salerno within the CRUI-CARE Agreement.

References

1 J. M. Millican and S. Agarwal, *Macromolecules*, 2021, **54**, 4455–4469.
2 G. L. Gregory, E. M. Lopez-Vidal and A. Buchard, *Chem. Commun.*, 2017, **53**, 2198–2217.
3 X. Zhang, M. Fevre, G. O. Jones and R. M. Waymouth, *Chem. Rev.*, 2018, **118**, 839–885.
4 S. C. Kosloski-Oh, Z. A. Wood, Y. Manjarrez, J. P. de los Rios and M. E. Fieser, *Mater. Horiz.*, 2021, **8**, 1084–1129.
5 K. Dutt and R. K. Soni, *Polym. Sci., Ser. B*, 2013, **55**, 430–452.
6 M. Brzezinski and M. Basko, *Molecules*, 2023, **28**, 1386.
7 R. H. Platel, L. M. Hodgson and C. K. Williams, *Polym. Rev.*, 2008, **48**, 11–63.
8 S. Paul, Y. Zhu, C. Romain, R. Brooks, P. K. Saini and C. K. Williams, *Chem. Commun.*, 2015, **51**, 6459–6479.
9 J. Gao, D. Zhu, W. Zhang, G. A. Solan, Y. Ma and W.-H. Sun, *Inorg. Chem. Front.*, 2019, **6**, 2619–2652.
10 A. Hermann, S. Hill, A. Metz, J. Heck, A. Hoffmann, L. Hartmann and S. Herres-Pawlis, *Angew. Chem., Int. Ed.*, 2020, **59**, 21778–21784.
11 D. M. Lyubov, A. O. Tolpygin and A. A. Trifonov, *Coord. Chem. Rev.*, 2019, **392**, 83–145.
12 R. W. F. Kerr, P. M. D. A. Ewing, S. K. Raman, A. D. Smith, C. K. Williams and P. L. Arnold, *ACS Catal.*, 2021, **11**, 1563–1569.
13 J. M. Longo, M. J. Sanford and G. W. Coates, *Chem. Rev.*, 2016, **116**, 15167–15197.
14 M. Hirschmann, F. Andriani and T. Fuoco, *Eur. Polym. J.*, 2023, **183**, 111766–111773.
15 O. Santoro, L. Izzo and F. Della Monica, *Sustainable Chem.*, 2022, **3**, 259–285.
16 S. Enthaler, *ACS Catal.*, 2013, **3**, 150–158.
17 S. Matsunaga and M. Shibasaki, *Chem. Commun.*, 2014, **50**, 1044–1057.
18 A. B. Kremer and P. Mehrkhodavandi, *Coord. Chem. Rev.*, 2019, **380**, 35–57.
19 L.-J. Wu, W. Lee, P. Kumar Ganta, Y.-L. Chang, Y.-C. Chang and H.-Y. Chen, *Coord. Chem. Rev.*, 2023, **475**, 214847.
20 C. K. Williams, N. R. Brooks, M. A. Hillmyer and W. B. Tolman, *Chem. Commun.*, 2002, 2132–2133.
21 P. D. Knight, A. J. P. White and C. K. Williams, *Inorg. Chem.*, 2008, **47**, 11711–11719.
22 S. Soobrattee, X. Zhai, K. Nyamayaro, C. Diaz, P. Kelley, T. Ebrahimi and P. Mehrkhodavandi, *Inorg. Chem.*, 2020, **59**, 5546–5557.
23 T. S. Hollingsworth, R. L. Hollingsworth, T. Rosen and S. Groysman, *RSC Adv.*, 2017, **7**, 41819–41829.
24 E. Bukhaltsev, L. Frish, Y. Cohen and A. Vigalok, *Org. Lett.*, 2005, **7**, 5123–5126.
25 Y. Sun, Y. Cui, J. Xiong, Z. Dai, N. Tang and J. Wu, *Dalton Trans.*, 2015, **44**, 16383–16391.
26 W.-L. Kong and Z.-X. Wang, *Dalton Trans.*, 2014, **43**, 9126–9135.
27 C. Romain, M. S. Bennington, A. J. P. White, C. K. Williams and S. Brooker, *Inorg. Chem.*, 2015, **54**, 11842–11851.
28 A. Thevenon, C. Romain, M. S. Bennington, A. J. P. White, H. J. Davidson, S. Brooker and C. K. Williams, *Angew. Chem., Int. Ed.*, 2016, **55**, 8680–8685.
29 S. Ghosh, Y. Schulte, C. Woelper, A. Tjaberings, A. H. Groeschel, G. Haberhauer and S. Schulz, *Organometallics*, 2022, **41**, 2698–2708.

30 M. Tansky and R. J. Comito, *Dalton Trans.*, 2023, **52**, 8784–8791.
31 Z.-T. Liu, C.-Y. Li, J.-D. Chen, W.-L. Liu, C.-Y. Tsai and B.-T. Ko, *J. Mol. Struct.*, 2017, **1134**, 395–403.
32 Y. Zhu, C. Romain, V. Poirier and C. K. Williams, *Macromolecules*, 2015, **48**, 2407–2416.
33 C. Romain and C. K. Williams, *Angew. Chem., Int. Ed.*, 2014, **53**, 1607–1610.
34 L. E. Breyfogle, C. K. Williams, V. G. Young Jr., M. A. Hillmyer and W. B. Tolman, *Dalton Trans.*, 2006, 928–936.
35 C.-H. Chang, H.-J. Chuang, T.-Y. Chen, C.-Y. Li, C.-H. Lin, T.-Y. Lee, B.-T. Ko and H.-Y. Huang, *J. Polym. Sci., Part A: Polym. Chem.*, 2016, **54**, 714–725.
36 P. K. Saini, G. Fiorani, R. T. Mathers and C. K. Williams, *Chem. – Eur. J.*, 2017, **23**, 4260–4265.
37 C.-Y. Yu, H.-J. Chuang and B.-T. Ko, *Catal. Sci. Technol.*, 2016, **6**, 1779–1791.
38 A. Thevenon, J. A. Garden, A. J. P. White and C. K. Williams, *Inorg. Chem.*, 2015, **54**, 11906–11915.
39 P. K. Saini, C. Romain, Y. Zhu and C. K. Williams, *Polym. Chem.*, 2014, **5**, 6068–6075.
40 F. Tufano, F. Santulli, F. Grisi and M. Lamberti, *ChemCatChem*, 2022, **14**, e202200962.
41 F. Santulli, G. Gravina, M. Lamberti, C. Tedesco and M. Mazzeo, *Mol. Catal.*, 2022, **528**, 112480.
42 F. Santulli, M. Lamberti and M. Mazzeo, *ChemSusChem*, 2021, **14**, 5470–5475.
43 A. Pilone, M. Lamberti, M. Mazzeo, S. Milione and C. Pellecchia, *Dalton Trans.*, 2013, **42**, 13036–13047.
44 I. D'Auria, M. Lamberti, M. Mazzeo, S. Milione, G. Roviello and C. Pellecchia, *Chem. – Eur. J.*, 2012, **18**, 2349–2360.
45 F. Santulli, F. Bruno, M. Mazzeo and M. Lamberti, *ChemCatChem*, 2023, **15**, e202300498.
46 M. Cozzolino, F. Melchionno, F. Santulli, M. Mazzeo and M. Lamberti, *Eur. J. Inorg. Chem.*, 2020, **2020**, 1645–1653.
47 Following the suggestion of a reviewer, a DOSY experiment was also carried out for the bimetallic complex **2** (Fig. S5 in the ESI†). The estimated molecular mass was in good agreement with the expected MM for the bimetallic mononuclear complex **2**.
48 D. E. Stasiw, A. M. Luke, T. Rosen, A. B. League, M. Mandal, B. D. Neisen, C. J. Cramer, M. Kol and W. B. Tolman, *Inorg. Chem.*, 2017, **56**, 14366–14372.
49 F. Isnard, M. Lamberti, L. Lettieri, I. D'Auria, K. Press, R. Troiano and M. Mazzeo, *Dalton Trans.*, 2016, **45**, 16001–16010.
50 A. A. Rosatella, S. P. Simeonov, R. F. M. Frade and C. A. M. Afonso, *Green Chem.*, 2011, **13**, 754–793.
51 T. Buntara, S. Noel, P. H. Phua, I. Melian-Cabrera, J. G. de Vries and H. J. Heeres, *Angew. Chem., Int. Ed.*, 2011, **50**, 7083–7087.
52 A. Arbaoui and C. Redshaw, *Polym. Chem.*, 2010, **1**, 801–826.
53 F. Isnard, M. Carratu, M. Lamberti, V. Venditto and M. Mazzeo, *Catal. Sci. Technol.*, 2018, **8**, 5034–5043.
54 E. Mahmoud, D. A. Watson and R. F. Lobo, *Green Chem.*, 2014, **16**, 167–175.
55 C. Robert, F. de Montigny and C. M. Thomas, *ACS Catal.*, 2014, **4**, 3586–3589.
56 M. Winkler, C. Romain, M. A. R. Meier and C. K. Williams, *Green Chem.*, 2015, **17**, 300–306.
57 C. Romain, J. A. Garden, G. Trott, A. Buchard, A. J. P. White and C. K. Williams, *Chem. – Eur. J.*, 2017, **23**, 7367–7376.
58 A. Arbaoui, C. Redshaw and D. L. Hughes, *Chem. Commun.*, 2008, 4717–4719.
59 Y.-H. Chen, Y.-J. Chen, H.-C. Tseng, C.-J. Lian, H.-Y. Tsai, Y.-C. Lai, S. C. N. Hsu, M. Y. Chiang and H.-Y. Chen, *RSC Adv.*, 2015, **5**, 100272–100280.